Dysregulation of Neuropilin-2 Expression in Inhibitory Neurons Impairs Hippocampal Circuit Development Leading to Autism-Epilepsy Phenotype

Vijjayalakshmi Santhakumar (vijayas@ucr.edu)
University of California Riverside https://orcid.org/0000-0001-6278-4187
Deepak Subramanian
Carol Eisenberg
https://orcid.org/0000-0002-8367-8671
Andrew Huang
Jiyeon Baek
https://orcid.org/0000-0002-6746-5086
Haniya Naveed
Samiksha Komatireddy
Michael Shiflett
Tracy Tran

Article

Keywords: Epilepsy, autism spectrum disorder, interneuron, GABA, CA1

Posted Date: February 9th, 2024

DOI: https://doi.org/10.21203/rs.3.rs-3922129/v1

Additional Declarations: The authors have declared there is **NO** conflict of interest to disclose

Abstract

Dysregulation of development, migration, and function of interneurons, collectively termed interneuronopathies, have been proposed as a shared mechanism for autism spectrum disorders (ASDs) and childhood epilepsy. Neuropilin-2 (Nrp2), a candidate ASD gene, is a critical regulator of interneuron migration from the median ganglionic eminence (MGE) to the pallium, including the hippocampus. While clinical studies have identified Nrp2 polymorphisms in patients with ASD, whether dysregulation of Nrp2-dependent interneuron migration contributes to pathogenesis of ASD and epilepsy has not been tested. We tested the hypothesis that the lack of Nrp2 in MGE-derived interneuron precursors disrupts the excitation/inhibition balance in hippocampal circuits, thus predisposing the network to seizures and behavioral patterns associated with ASD. Embryonic deletion of Nrp2 during the developmental period for migration of MGE derived interneuron precursors (iCKO) significantly reduced parvalbumin, neuropeptide Y, and somatostatin positive neurons in the hippocampal CA1. Consequently, when compared to controls, the frequency of inhibitory synaptic currents in CA1 pyramidal cells was reduced while frequency of excitatory synaptic currents was increased in iCKO mice. Although passive and active membrane properties of CA1 pyramidal cells were unchanged, iCKO mice showed enhanced susceptibility to chemically evoked seizures. Moreover, iCKO mice exhibited selective behavioral deficits in both preference for social novelty and goal-directed learning, which are consistent with ASD-like phenotype. Together, our findings show that disruption of developmental Nrp2 regulation of interneuron circuit establishment, produces ASD-like behaviors and enhanced risk for epilepsy. These results support the developmental interneuronopathy hypothesis of ASD epilepsy comorbidity.

Introduction

Autism spectrum disorders (ASD) and epilepsy are highly comorbid conditions that are proposed to share common pathophysiological mechanisms. Anomalies in the development, migration, and function of interneurons, collectively termed interneuronopathies, are closely associated with ASD and epilepsy (1–4). In particular, the development of seizures and behavioral impairments observed in ASD are associated with altered function of inhibitory neurons. GABAergic interneurons play a pivotal role in the organization and function of the hippocampus, a brain region frequently associated with ASD and epilepsy (5, 6). Disruptions in the establishment of interneuron circuits can compromise hippocampal network function, potentially serving as a common factor contributing to the observed high comorbidity between ASD and epilepsy (7–12). Here we report that developmental dysregulation of a classical guidance cue receptor Neuropilin-2 (Nrp2) specifically in developing interneurons compromises hippocampal circuit function and predisposes the network to seizures and behavioral deficits consistent with ASD.

During embryonic development, the class 3 secreted semaphorins and their obligate binding receptors, the neuropilins, are key regulators of neuronal migration, axonal guidance, dendritic morphology, and synaptic specificity of various cell types (13–15). Notably, Nrp2 is a candidate ASD gene on SFARI (Score 2) and polymorphisms in Nrp2 gene have been reported in patients with autistic syndromes (16, 17). In excitatory neurons, Nrp2 expression contributes to pruning of synapses, spines and axons, whereas, in

inhibitory neurons, Nrp2 regulates migration of interneurons from the medial ganglionic eminence (MGE) to the pallium, including the hippocampus (18–20). During embryonic development, the expression of Nrp2 in interneuron progenitors is tightly regulated by the transcription factor Nkx2.1 (21), and allows for migration of parvalbumin (PV+), somatostatin (SOM+) and neuropeptide-Y (NPY+) expressing interneurons to the cortex and hippocampus (22). We previously found that global constitutive knockout of Nrp2 leads to loss of hippocampal interneurons, produces behavioral phenotypes consistent with ASD, and increases seizure susceptibility (23, 24). However, whether selective deletion of Nrp2 in interneurons alone and during their time of migration to the cortex and hippocampus could result in ASD/epilepsy phenotypes is currently not known. We hypothesize that loss of Nrp2 during embryonic ages (E12.5-13.5) specifically in interneuron precursors derived from the MGE will result in fewer inhibitory neurons in the hippocampus. We predict that the ensuing altered inhibition and related circuit plasticity will disrupt hippocampal function, increase seizure susceptibility, and impair hippocampal-dependent behaviors. To test these hypotheses, we deleted Nrp2 in MGE-derived interneuron precursors by crossing the Nrp2 flox conditional mouse with the Nkx2.1-CreERT2 driver line, where cre recombinase expression is induced by tamoxifen administered to pregnant dams on E12.5 and E13.5. The resulting genotype *Nrp2*$^{f/f}$;*Nkx2.1-Cre*$^{+}$ (iCKO) animals and littermate controls were used to examine hippocampal CA1 circuit functions and evaluated whether the lack of Nrp2 in interneuron precursors enhances the risk for development of seizures and behavioral deficits consistent with ASD.

Materials and Methods

Animals

All experiments were performed in accordance with IACUC protocols approved by Rutgers University, Newark, NJ, and the University of California at Riverside, CA and in keeping with the ARRIVE guidelines. The *Nrp2* floxed mouse (25), which contains an IRES-GFP-polyA sequence inserted immediately downstream of the 3' loxP in the targeting construct that allows the expression of GFP following cre recombination in all conditional mutant (-/-) neurons, was crossed with the *Nkx2.1-CreERT2* mouse (stock #014552, The Jackson Laboratory), to selectively target MGE-derived interneuron progenitors during embryonic development(21) (See Fig. 1A). Cre recombinase was induced by administering tamoxifen (5 mg, by oral gavage) to the pregnant dams at E12.5 and E13.5, during the peak timeline for developmental interneuron migration (Fig. 1B). Deletion of *Nrp2* in the progeny (*Nrp2*$^{f/f}$;*Nkx2.1Cre*$^{+}$*)* resulted in inhibitory conditional knockout (iCKO) mice and was verified by visualization of GFP expression in the hippocampus in adult mice (Fig. 1C&D). All appropriate littermates, such as Cre negative *Nrp2*$^{+/f}$;*Cre*$^{-}$ *or Nrp2*$^{f/f}$;*Cre*$^{-}$ and *Nrp2*$^{+/+}$;*Cre*$^{+}$, were used as controls. In immunostaining and behavioral studies, data from *Nrp2*$^{+/f}$;*Cre*$^{+}$ mice were not statically different from Cre negative controls or *Nrp2*$^{+/+}$;*Cre*$^{+}$ mice and were pooled for analysis. Mice used in these studies were backcrossed for at least 10 generations to the *C57BL/6NTac* background strain. *Nrp2* genotypes were confirmed by using polymerase chain reaction (PCR).

Immunostaining and cell count:

Immunostaining, cell counts, and photo-documentation are as detailed previously in Eisenberg et al 2021(24) and described in detail in Supplementary Methods.

Ex vivo physiology:

Whole-cell patch clamp recordings of CA1 pyramidal cells (CA1 PCs) were obtained from horizontal hippocampal slices (350µm) of littermate controls (*Nrp2*$^{+/f}$;*Cre*$^{-}$ *or Nrp2*$^{f/f}$;*Cre*$^{-}$*)* and iCKO mice (*Nrp2*$^{f/f}$;*Nkx2.1Cre*$^{+}$; n = 3 animals/group, 12 months old). Slice preparation and recording methods are as detailed previously (24, 26). Voltage and current clamp recordings were obtained using MultiClamp 700B amplifiers, digitized at 10kHz using DigiData 1440A or DigiData 1550B and recorded using pClamp10 software (Molecular Devices, Sunnyvale, CA). Active and passive properties were recorded in current clamp from a holding potential of -70mV using K-Gluconate based internal solution. Voltage clamp recording from CA1 PCs held at -70mV and 0mV were used to isolate glutamatergic and GABAergic synaptic inputs, respectively, using a Cesium-based internal solution. Action potential independent miniature currents were isolated by tetrodotoxin (TTX, 1µM). Intrinsic properties were analyzed using pClamp software 10.7 (Molecular Devices, Sunnyvale, CA) and synaptic currents were detected using template search feature in Easy Electrophysiology (version 2.6).

In vivo electrophysiology:

Eight mice (5 *Nrp2*$^{+/f}$;*Cre*$^{-}$ *or Nrp2*$^{f/f}$;*Cre*$^{-}$ littermate controls and *3 Nrp2*$^{f/f}$;*NkxCre*$^{+}$; average age of 8.75 ± 0.70 months, five males and three females) were surgically implanted a tungsten wire depth electrode (50 µm, California Fine Wire company) in the CA1 subfield (AP:2 mm, ML: 1.5 mm, DV: 1.2mm from bregma) and a cortical screw electrode. Two additional screw electrodes (Invivo1, Roanoke, VA) on the contralateral hemisphere served as ground and reference. After 3–5 days of recovery, mice were connected to a tethered video-EEG monitoring system. Signals were sampled at 10 kHz, amplified (preamplifier: 8202-SE3, gain – x100, Pinnacle Technologies, Lawrence, KS), digitized (Powerlabs16/35, AD Instruments, Colorado Springs, CO), and recorded using LabChart 8.0 (AD instruments). Following 30 minutes of baseline recordings, mice received a single high dose of KA (20 mg/kg), and their latency to electrographic seizure, seizure duration, and mortality were quantified. Seizures were scored by a blinded investigator (S.K) based on a modified Racine scale. Seizure severity scores in the first 30 min were averaged over 5 min epochs.

Behavior testing

The behavior methods are fully described in the supplemental methods and in previous publications (23)

Social novelty test

We assessed social behavior in a three-chambered arena. In the first phase, one chamber contained a caged mouse, the opposite chamber contained an empty cage, and the test mouse was able to explore both chambers. During the test for social novelty, which was conducted immediately following the first

phase, one chamber contained the familiar mouse used previously, and the opposite chamber contained a novel mouse. In both phases, the test mouse explored the arena for 5 minutes. We assessed time spent sniffing the novel and familiar mouse from video footage.

Novel object recognition test

The test mouse explored two identical objects in an open field arena for 10 minutes. After a 30-min retention interval, the mouse reentered the arena, which contained an object they previously encountered (familiar object) and a novel object. Two observers blind to experimental conditions assessed time spent sniffing the novel and familiar objects from video footage.

Instrumental goal directed behavior test

We tested mice on an instrumental goal-directed learning task. Food-restricted mice pressed levers to obtain food pellets. Responses on one lever delivered chocolate-flavored pellets, whereas responses on the opposite lever delivered grain pellets. Mice underwent 36 instrumental training sessions, two sessions per day, with each lever trained in separate sessions. Mice then underwent a selective-satiety outcome devaluation procedure, in which they had free access to one flavor of food pellets in their home cage for 1 hour. In the choice test that followed, both levers were available, and mice could respond for 5 minutes, with no pellets delivered during the test. After 4 retraining sessions, we repeated the test with the opposite outcome devalued prior to the choice test.

Statistical analysis

Unpaired *t*-tests, two-way ANOVA and post hoc Bonferroni's, Sidak's or Tukey's multiple comparison correction were used to compare cell count and behavioral data. Kolmogorov-Smirnov test for cumulative distributions was used to evaluate differences in distribution of synaptic parameters. Unpaired students *t*-test was used to compare differences in intrinsic properties, latency to convulsive seizures and the total time spent in seizures. Mantel-Cox test was used for survival analysis. All statistical tests were conducted in GraphPad Prism.

The difference between two dependent means (matched pairs) was used to determine the sample size requirement of behavioral tests using G*Power 3.1 software. A sample size requirement of three to seven animals for cell counts and 5 to 8 for behavior testing was estimated by using 80% power and an effect size found in previous work and literature. Exclusion criteria of three standard deviations from the mean was pre-established for behavior tests. One mutant mouse performed over three standard deviations lower than the mean and was therefore eliminated from behavior analysis. Significance was set to $p < 0.05$. Data are shown as mean ± SEM or median and interquartile range (IQR), as appropriate.

Results

Developmental deletion of Nrp2 in interneuron progenitors reduces hippocampal interneuron density.

Previously, Nrp2 was shown to be expressed in MGE derived interneuron precursors and is critical for cortical and hippocampal migration of interneurons (20, 28). To examine the impact of Nrp2 expression in inhibitory neuron precursors on hippocampal circuit formation and function, we generated the *Nrp2*$^{f/f}$;*Nkx2.1-CreERT2*$^{+}$ (iCKO), where cre recombinase expression is induced by feeding the pregnant dams with tamoxifen on E12.5 and E13.5 (Fig. 1A-B). Induction of cre-recombinase was confirmed by GFP expression in the hippocampus of the iCKO mice, as the *Nrp2* flox contained an IRES-GFP-pA sequence that will be shifted in frame to be transcribed upon cre recombination, but not in littermate controls (Fig. 1C-D).

To understand the effects of Nrp2 deletion on the distribution of different MGE derived hippocampal inhibitory neuron subtypes, we quantified the population of PV+, SOM + and NPY + expressing interneurons in hippocampal subfields of iCKO mice. We particularly focused on the CA1 subfield, a region closely associated with storing social memories and pathologically implicated in ASD (29, 30). Soma targeting PV + interneurons are estimated to account for 21% of MGE-derived interneurons (31). Selective deletion of Nrp2 led to a 32.91% decrease in hippocampal PV + interneurons population compared to control mice (Fig. 1E-J, PV neurons / section, littermate control: 52.06 ± 4.56; iCKO: 39.17 ± 1.81; n = 5 mice, averaged over 10 sections in each, p = 0.03; $t_{(8)}$ = 2.629 unpaired *t*-test). In the CA1 region, we observed a 24.54% decrease in PV + neuron population (mean cell count control: 22.04 ± 1.61; iCKO: 16.63 ± 0.81 in n = 5 mice each p = 0.01; $t_{(32)}$ = 3.176 by two-way ANOVA with Bonferroni multiple comparison correction). We did not observe a difference in PV + neurons in other hippocampal subfields including dentate gyrus (DG), CA2 and CA3.

Dendrite targeting SOM + neurons are important in regulating dendritic inputs and MGE-derived interneurons account for approximately 60% of SOM + neuron population in the hippocampus (31). Following deletion of Nrp2, we observed a 37.12% decrease in overall hippocampal SOM + population (Fig. 2A-F; cell count, control: 84.03 ± 7.88; iCKO: 52.83 ± 7.50, p = 0.0426; $t_{(6)}$ = 2.565 unpaired *t*-test). In the CA1 we observed a substantial 46.41% decrease in SOM + neurons (cell count: control: 36.90 ± 3.97; iCKO: 19.78 ± 3.14 in n = 5 mice each p = 0.0004; $t_{(24)}$ = 4.659 by two-way ANOVA with Bonferroni multiple comparison correction). Interestingly, there was an apparent reduction in SOM + cells in the DG, but the difference did not reach statistical significance (p = 0.385). We did not observe any differences in SOM + cells in CA2 and CA3 subfields of the hippocampus.

We next quantified the population of NPY + expressing interneurons which contribute to shaping synchronized activity in hippocampal circuits (32, 33). We observed a 40.7% decrease in total NPY + expressing interneurons in the hippocampus. (Fig. 2G-L; mean cell count: controls: 80.63 ± 3.30; iCKO: 47.83 ± 1.93, n = 5 each p = 0.0003; $t_{(6)}$ = 7.674 unpaired *t*-test). In the CA1 subfield, we observed a 49.02% decrease in NPY + neurons (mean cell count: controls: 33.90 ± 3.10; iCKO: 17.01 ± 1.81, $t_{(24)}$ = 6.519; two-way ANOVA with Bonferroni multiple comparison correction p < 0.0001). In other subfields including DG, CA2 and CA3, we observed a trend towards a decrease in NPY + neurons (p = 0.2135, p = 0.4776 and p = 0.0755 respectively) which did not reach statistical significance.

Together, our results show a significant decrease in PV+, SOM + and NPY + interneuron population in the CA1 following developmental deletion of Nrp2 in MGE-interneuron precursors. This reduction in interneuron populations supporting perisomatic and dendritic feedback inhibition is likely to have functional consequences at a neuronal and network level which we examined further.

Developmental Nrp2 deletion in interneurons alters inhibitory and excitatory synaptic transmission in CA1.

Altered excitation / inhibition balance is considered a fundamental pathophysiological mechanism affecting cortical and hippocampal function in ASD (7, 8). Decrease in interneuron populations in CA1 can alter basal inhibitory control of CA1 pyramidal cells (PCs) and lead to compensatory changes. We examined whether action potential dependent spontaneous inhibitory currents and action potential independent miniature inhibitory synaptic inputs to CA1 were affected in iCKO mice. Voltage clamp recordings of spontaneous inhibitory postsynaptic currents (sIPSCs) in CA1 PCs revealed a significant increase in interevent intervals (IEI), indicating a decrease frequency in iCKO mice (Fig. 3A,B, sIPSC interevent intervals in ms, controls: 115.3 ± 4.57, median: 71.40, IQR: 35.0–150.9, n = 8 cells from 3 mice; iCKO: 133.6 ± 4.82, median: 87.65, IQR: 42.2–166.9, n = 9 cells from 3 mice; p = 0.0037 by Kolmogorov-Smirnov test, Cohen's D: 0.13). However, iCKO mice showed an increase in sIPSC amplitude compared to control mice (Fig. 3B boxed inset; in pA: controls: 17.56 ± 1.086, median: 15.51, IQR: 12.46–21.23, iCKO: 22.29 ± 1.059, median: 20.30, IQR 16.04–25.51; n = 8 vs 9 cells from 3 mice; p < 0.0001 by Kolmogorov-Smirnov test, Cohen's D: 0.50). While reduction in sIPSC frequency could potentially arise due reduced interneuron population in the CA1, increase in sIPSC amplitude suggests homeostatic synaptic scaling in iCKO mice (34). Further examination of action potential independent miniature currents (mIPSC) also revealed a significant increase in interevent intervals (decrease in frequency) in iCKO mice indicating a potential decrease in inhibitory neuron synapses on to CA1 PCs or release probability (Fig. 3C-D; mIPSC IEI in ms, controls: 88.79 ± 3.04, median: 68.45, IQR: 33.53–113.1, n = 8 cells from 3 mice; iCKO : 126.5 ± 4.87, median: 85.40, IQR: 45.13–163.9, n = 7 cells from 3 mice; p < 0.0001 by Kolmogorov-Smirnov test, Cohen's D: 0.37). Unlike sIPSC amplitude, there was a decrease in mIPSC amplitude in iCKO mice (Fig. 3D boxed inset; in pA: control: 17 ± 0.25, median: 15.45, IQR 11.88–20.41, iCKO: 18.05 ± 0.29, median: 16.65, IQR 12.94–21.28, p < 0.001 by Kolmogorov-Smirnov test, Cohen's D: 0.14). Together our data show a significant reduction in spontaneous and miniature inhibitory inputs to CA1 PCs in iCKO mice.

Impaired inhibitory control of CA1 PCs can augment network excitability or lead to compensatory/homeostatic plasticity (34). To determine if the reduction in inhibition altered excitatory drive to PCs, we evaluated genotype specific differences in sEPSC frequency and amplitude in CA1 PCs. Contrary to expectations based on homeostatic plasticity, CA1 PCs from iCKO mice showed an increase in the frequency of sEPSCs compared to controls. (Fig. 4A-B; sEPSC interevent intervals in ms: controls: 1424 ± 59.22, median: 765.7, IQR: 250.2–1872, n = 9 cells from 3 mice; iCKO: 1145 ± 44.28, median: 698.4, IQR: 265.7–1563, n = 9 cells from 3 mice; p = 0.0243 by Kolmogorov-Smirnov test, Cohen's D: 0.17). However, sEPSC amplitude was not statistically different between groups (Fig. 4B boxed inset; in pA, controls: 17.34 ± 1.127, iCKO: 17.29 ± 0.902, n = 9 cells from 3 mice/group). Together, our findings

demonstrate a deficit in basal inhibitory inputs and a potentially maladaptive increase in excitatory inputs which could act in concert to enhance CA1 network excitability in iCKO mice.

Nrp2 deletion in interneurons does not affect intrinsic physiology of CA1 PCs.

Homeostatic tuning of neuronal intrinsic properties often occurs to stabilize circuit function (35). Our findings show significant changes in inhibitory circuit function along with an increase in excitatory inputs in CA1 subfield after *Nrp2* deletion. Therefore, we evaluated whether the synaptic changes were accompanied by alterations in intrinsic active and passive properties of CA1 PCs. In current clamp recordings, CA1 PCs (Fig. 4C) showed no differences in the frequency of action potential firing in response to step current injections (Fig. 4D-E). Although, firing threshold of CA1 PC's were not different between control and iCKO mice, action potential amplitude was significantly increased (Fig. 4F; Action potential threshold in mV: controls − 42.58 ± 1.03, iCKO: -44.25 ± 1.44; amplitude in mV: controls 78.32 ± 1.72, iCKO 89.36 ± 2.55, *n* = controls 15 cells from 3 mice, iCKO 11 cells from 3 mice, $p = 0.0011$, $t_{(24)} = 3.722$ unpaired *t*-test). However, spike frequency adaptation and fast afterhyperpolarization (fAHP) in iCKO mice was not different from control (Supplementary Fig. 1A-B, Spike frequency adaptation: controls 0.771 ± 0.086, iCKO: 0.582 ± 0.120; n = controls 15 cells from 3 mice, iCKO 11 cells from 3 mice). Examining passive membrane properties revealed no differences in resting membrane potential (RMP), input resistance (Rin), and sag ratio between controls and iCKO mice (Fig. 4F and supplementary Fig. 1C. RMP in mV, control: -69.07 ± 0.658; iCKO: -67.64 ± 1.370; Rin in MΩ, control: 113.9 ± 5.415, iCKO: 121.5 ± 6.124; Sag Ratio: controls 0.955 ± 0.003, iCKO: 0.954 ± 0.003; *n* = controls 15 cells from 3 mice, iCKO 11 cells from 3 mice). These results demonstrate that CA1 PC active and passive intrinsic properties are mostly unchanged by selective deletion of *Nrp2* in interneurons.

Selective deletion of Nrp2 in interneurons increases risk for seizures.

Since our experiments consistently show a decrease in interneuron population, network inhibition and increased excitatory neurotransmission, we examined if this could result in increased seizure susceptibility. Interestingly, we noticed an increase in mortality specifically in iCKO mice after electrode implant (n = 3 of 6). Nevertheless, we did not observe spontaneous seizures or epileptiform activity in iCKO mice during the brief 30 min baseline recording period. iCKO mice injected with a single convulsive dose of KA (20mg/kg, i.p) showed a significantly shorter latency to develop convulsive seizures and reached status epilepticus more rapidly (Fig. 5A-B; latency in minutes, Controls: 27.7 ± 3.27, n = 5; iCKO: 4.8 ± 1.95, *n* = 5 vs 3, $p = 0.0025$, $t_{(6)} = 4.993$ unpaired *t*-test). At 30 minutes post injection, all iCKO mice reached stage 4 seizures, classified using a modified Racine scale whereas, only 1 control mouse exhibited stage 4 seizure. Moreover, iCKO mice showed a 100% mortality within the first 60 minutes of KA induction whereas all control animals survived this period (Fig. 5C; Mean latency to mortality in iCKO mice: 27.02 ± 12.22 minutes, p = 0.022, Mantel-Cox Test). Importantly, iCKO mice spent ~ 60% of their time after KA injection exhibiting behavioral seizures compared to controls (Fig. 5D, measured as total time spent in convulsive seizures/total time from induction to death or 60 minutes: Controls: 19.78 ±

4.42%; iCKO: 60.69 ± 3.12%, $n = 5$ vs 3, $p < 0.001$, $t_{(6)} = 6.483$, unpaired t-test). Together, our experiments demonstrate iCKO mice exhibit greater seizure susceptibility than controls.

Social novelty and goal directed behaviors are impaired in mice with interneuron targeted Nrp2 deletion.

Given *Nrp2*'s association with ASD in humans, and our previous results showing social, learning, and sensorimotor alterations in *Nrp2*-null mice, we examined ASD-relevant behaviors in iCKO mice. We found that preference for social novelty, measured as the proportion of time spent investigating a novel versus a familiar mouse, was impaired in iCKO mice compared to littermate controls (Fig. 6A). Unlike control mice, which showed a significant preference for the novel mouse, iCKO mice showed no preference for social novelty (Fig. 6B; two-way ANOVA interaction $F_{(1,36)} = 6.388$, $p = 0.0110$; n = 11 controls and 9 iCKO mice). Further analysis failed to reveal genotype specific differences in overall investigation time (in sec, control = 110 ± 21 sec; iCKO = 94 ± 25 sec) indicating that the difference in responses is not due to an overall lack of interest in social interactions.

Since social preference test relies on memory of previous encounters, we tested whether deficits in episodic memory could have contributed to deficits in social novelty preference in iCKO mice. However, iCKO mice did not differ from control mice in an object recognition memory test (Fig. 6C), indicating that the lack of preference for social novelty reflects a specific change in social behavior in iCKO mice.

In addition to changes in social behavior, iCKO mice differed from control mice in goal-directed behavior (Fig. 6D) in an instrumental lever press task with two actions associated with two distinct food outcomes. Devaluation of one instrumental outcome significantly shifted the choice of the control mouse to the action (lever press) associated with the valued outcome, whereas the actions of iCKO mice showed no sensitivity to changes in outcome value (Fig. 6E; two-way ANOVA interaction $F_{(1,26)} = 8.265$ $p < 0.0001$; $n =$ 7 controls and 8 iCKO). Importantly, iCKO mice and controls did not differ in acquisition of the instrumental response (Fig. 6F) demonstrating iCKO mice were capable of acquiring and performing a lever press action and showed no learning deficits. Similarly, locomotor measures in the open field and accelerating rotarod were not different between iCKO mice and controls (Supplementary Fig. 2A-B) indicating lack of motor impairments. Moreover, control and iCKO mice did not differ in the time spent in open arm of the elevated-zero maze or grooming behavior (Supplementary Fig. 2C-D) revealing iCKO mice were not more anxious than controls. Therefore, the inability to adjust actions to changes in outcome value in iCKO mice strongly suggest a selective impairment in control of goal-directed actions.

Together, these findings suggest that Nrp2-dependent interneuron circuit development is a critical factor determining proper social behavior and cognitive flexibility in mice, and deficits in Nrp2 during development can significantly impair these functions.

Discussion

Dysregulated excitatory/inhibitory (E/I) balance is often considered a unifying pathology underlying Autism-Epilepsy comorbidity. Altered functional connectivity, loss of interneurons or hypoactive

interneurons have been proposed to underlie this shift in functional E/I balance (8). The emerging role of interneurons as critical determinants of circuit dysfunction in ASD is evident from studies in animal models and humans (2, 11). Despite this knowledge, the molecular determinants of altered inhibitory circuits during neurodevelopment and the impact of such maladaptive circuits on network and behavioral function are unknown. Neuropilin-2 and its interactions with its ligand the secreted semaphorin 3F are crucial in establishing normal migration of interneuron to the cortex, the lack of which has been shown to result in increased NPY + expressing interneurons in the striatum (20). Importantly, Nrp2 is a candidate ASD gene on SFARI (Score 2) and polymorphisms in Nrp2 gene have been reported in patients with autistic syndromes (16, 17). We previously demonstrated that global Nrp2 deletion results in a significant decrease in density of several MGE-derived interneuron subtypes in hippocampus and reduced hippocampal inhibition (24). However, the effects of selective embryonic Nrp2 deletion in MGE-derived interneuron precursors and its impact on hippocampal interneuron population and inhibition was unknown. The current studies directly address this gap in knowledge and demonstrate that embryonic deletion of Nrp2 selectively in MGE-derived interneuron precursors leads to a significant reduction in PV+, SOM + and NPY + interneurons in the hippocampus. The reduction in interneuron numbers in the hippocampus could result from mislocalization and result in altered interneuron numbers in other brain regions, such as the striatum or cortex. Alternatively, failure of MGE-derived precursors to their final destination could result in cell death, which future experiments, beyond the scope of this study, can examine.

At a circuit level, CA1 PCs from iCKO mice received a less frequent synaptic inhibition compared to control mice. This finding is similar to our observations in global *Nrp2* KO mice and could directly be attributed to the decrease in interneuron population in CA1. The absence of a GABAergic inhibitory tone is believed to reduce signal to noise ratio and disrupt signal processing in individuals with ASD (7, 8, 36). We identify reductions in three major interneuronal classes in the iCKO mice; the soma-targeting fast-spiking PV + basket cells and dendrite targeting SOM + interneurons which are crucial regulators of neuronal spiking and integration of information (37), and NPY + interneurons which are critical regulators of excitatory synaptic transmission and spiking frequency(38). Therefore, the combined reduction in their populations is likely to have a cumulative effect on network function leading to alterations in excitatory synaptic transmission, neuronal oscillations and theta/gamma coupling. Together, these changes could disrupt information processing and lead to behavioral deficits consistent with ASD (39). Despite the reduction in inhibition, we observed a significant increase in excitatory synaptic transmission in CA1 PCs from iCKO mice suggesting potential maladaptive plasticity. Moreover, while the deficits in inhibition in the iCKO mice are similar to those reported in the global *Nrp2* KO, the changes in CA1 PC excitability and resting membrane potential observed in the global *Nrp2* KO were not observed in the iCKO mice. Thus, our findings support the proposal that interneuron specific knockout of *Nrp2* undermines E/I balance at a circuit level predominantly through disruption of the fine-tuned, layer-specific inhibitory control of CA1.

Enhanced excitability and deficient inhibitory control are fundamental to seizures. iCKO mice exhibited higher susceptibility to evoked seizures compared to age matched controls. Importantly, the severity of evoked seizures in iCKO mice was high, leading to 100% mortality. Our findings that the iCKO mice also

spent ~ 60% of their time post-induction in seizures highlights their enhanced susceptibility to recurrent epileptic episodes.

Altered social behavior and impaired action control are core features of ASD. In iCKO mice, we observed a lack of preference for social novelty and an impairment in goal-directed behavior, consistent with an ASD phenotype. Preference for social novelty depends, in part, on hippocampal CA2 and its output to ventral CA1 (40, 41). Furthermore, studies have shown that disrupted E/I balance in CA2 interferes with social novelty preference and increases seizure susceptibility (42, 43). While the trend is not significant in the iCKO animals, we previously found in the *Nrp2* global KO mice a significant decrease of both PV + and SOM + interneurons in CA2 compared to the WT controls. Therefore, loss of social novelty preference in iCKO mice may reflect dysregulated interneuron migration to CA2 or reflect changes in interneuron number and function in ventral CA1 that receives CA2 input. Interestingly, iCKO mice showed no deficits in episodic memory as assessed in the novel object recognition test. These data indicate that the lack of preference for social novelty was not due to an impairment in episodic memory, or a lack of interest in novelty *per se.* The dependency of novel object recognition on hippocampus is debated, with more evidence in support of entorhinal cortex underlying performance in the novel object recognition task (44). We previously reported that *Nrp2* global KO animals were impaired in novel object recognition (23); however, global *Nrp2* KO mice also displayed increases in cortical pyramidal neuron dendritic spine number and excitability (18, 27), which may have affected entorhinal cortex processing and produced a deficit in the novel object recognition task. These findings further underscore the functional distinctions between effects of global versus inhibitory neuron specific *Nrp2* deletion.

Goal-directed action was also impaired in iCKO mice. In an instrumental outcome devaluation task, mice are given the choice of actions associated with either a valued or devalued outcome. Unlike control mice that chose the action associated with the valued outcome, iCKO mice showed no preference. The impairment in goal-directed response in iCKO mice may be attributable to altered hippocampal activity. The dorsal hippocampus is transiently involved in the formation of action-outcome associations (45, 46), which could have prevented mice from forming the associations necessary to guide their behavior in the devaluation test. Another possibility is that the altered interneuron migration induced in iCKO mice misplaced striatal interneurons (20). Disruption of striatal GABAergic interneurons impairs goal-directed behavior (47, 48), suggesting striatal deficits as a source of impaired goal-directed behavior in iCKO mice. Future studies will address Nrp2's role in striatal interneuron migration and its effects on behavior.

Taken together, our findings provide a novel insight into the circuit and behavioral effects of embryonic *Nrp2* deletion in interneuron precursors. Our studies using interneuron specific *Nrp2* deletion combined with circuit and behavioral analyses support a role for developmental interneuronopathy in comorbidity of ASD-epilepsy syndromes.

Declarations

Declaration of Interest:

None

Author contributions:

D. S., C.E., A.H., J.B., and H.N. performed experiments; D. S., C.E., A.H., M.W.S., V.S., and T.S.T. analyzed data and interpreted results of experiments; C.E., D.S., and A. H. prepared figures; M.W.S., V.S., and T.S.T. conception and design of research; D.S, C.E., M.W.S., V.S. and T.S.T. drafted manuscript.

Declaration of interest:

The authors have no known competing financial interests or personal relationships that could have appeared to influence the work reported in this paper.

Acknowledgements:

This work is supported by the NJ Governor's Council for Medical Research and Treatment of Autism: CAUT17BSP011 to V.S. and T.S.T., CAUT17BSP022 to T.S.T. and M.W.S., Rutgers Brain Health Initiative Pilot Grants to T.S.T. and V.S., NIH F31NS131052 and AES957615 to A.H., NIH R01 NS069861 and NS097750 to V.S., and NSF/IOS: 1556968 to T.S.T.

References

1. Katsarou A, Moshé SL, Galanopoulou AS. Interneuronopathies and their role in early life epilepsies and neurodevelopmental disorders. Epilepsia Open. 2017;2(3):284–306.
2. Contractor A, Ethell IM, Portera-Cailliau C. Cortical interneurons in autism. Vol. 24, Nature Neuroscience. Nature Research; 2021. p. 1648–59.
3. Brooks-Kayal A. Epilepsy and autism spectrum disorders: are there common developmental mechanisms? Brain Dev. 2010;32(9):731–8.
4. Ben-Ari Y. Is birth a critical period in the pathogenesis of autism spectrum disorders? Nature Reviews Neuroscience 2015 16:8. 2015;16(8):498–505.
5. Akerman CJ, Cline HT. Refining the roles of GABAergic signaling during neural circuit formation. Trends Neurosci. 2007;30(8):382–9.
6. Banker SM, Gu X, Schiller D, Foss-Feig JH. Hippocampal contributions to social and cognitive deficits in autism spectrum disorder. Trends Neurosci. 2021;44(10):793–807.
7. Rubenstein JLR, Merzenich MM. Model of autism: increased ratio of excitation/inhibition in key neural systems. Genes Brain Behav. 2003;2(5):255–67.
8. Sohal VS, Rubenstein JLR. Excitation-inhibition balance as a framework for investigating mechanisms in neuropsychiatric disorders. Mol Psychiatry. 2019;24(9):1248–57.
9. Nelson SB, Valakh V. Excitatory/Inhibitory Balance and Circuit Homeostasis in Autism Spectrum Disorders. Vol. 87, Neuron. Cell Press; 2015. p. 684–98.
10. Buckley AW, Holmes GL. Epilepsy and Autism. Cold Spring Harb Perspect Med. 2016;6(4):a022749.

11. Bozzi Y, Provenzano G, Casarosa S. Neurobiological bases of autism–epilepsy comorbidity: a focus on excitation/inhibition imbalance. European Journal of Neuroscience. 2018;47(6):534–48.
12. Gogolla N, LeBlanc JJ, Quast KB, Südhof TC, Fagiolini M, Hensch TK. Common circuit defect of excitatory-inhibitory balance in mouse models of autism. J Neurodev Disord. 2009;1(2):172–81.
13. Tran TS, Kolodkin AL, Bharadwaj R. Semaphorin regulation of cellular morphology. Annu Rev Cell Dev Biol. 2007;23:263–92.
14. Pasterkamp RJ. Getting neural circuits into shape with semaphorins. Nat Rev Neurosci. 2012;13(9):605–18.
15. Koropouli E, Kolodkin AL. Semaphorins and the dynamic regulation of synapse assembly, refinement, and function. Curr Opin Neurobiol. 2014;27:1–7.
16. Hosseinpour M, Mashayekhi F, Bidabadi E, Salehi Z. Neuropilin-2 rs849563 gene variations and susceptibility to autism in Iranian population: A case-control study. Metab Brain Dis. 2017;32(5):1471–4.
17. Wu S, Yue W, Jia M, Ruan Y, Lu T, Gong X, et al. Association of the neuropilin-2 (NRP2) gene polymorphisms with autism in Chinese Han population. Am J Med Genet B Neuropsychiatr Genet. 2007;144B(4):492–5.
18. Tran TS, Rubio ME, Clem RL, Johnson D, Case L, Tessier-Lavigne M, et al. Secreted semaphorins control spine distribution and morphogenesis in the postnatal CNS. Nature. 2009;462(7276):1065–9.
19. Riccomagno MM, Kolodkin AL. Sculpting Neural Circuits by Axon and Dendrite Pruning. Annu Rev Cell Dev Biol. 2015;31(1):779–805.
20. Marín O, Yaron A, Bagri A, Tessier-Lavigne M, Rubenstein JLR. Sorting of Striatal and Cortical Interneurons Regulated by Semaphorin-Neuropilin Interactions. Science (1979). 2001 Aug 3;293(5531):872–5.
21. Xu Q, Tam M, Anderson SA. Fate mapping Nkx2.1-lineage cells in the mouse telencephalon. Journal of Comparative Neurology. 2008;506(1):16–29.
22. Pleasure SJ, Anderson S, Hevner R, Bagri A, Marin O, Lowenstein DH, et al. Cell Migration from the Ganglionic Eminences Is Required for the Development of Hippocampal GABAergic Interneurons. Neuron. 2000;28(3):727–40.
23. Shiflett MW, Gavin M, Tran TS. Altered hippocampal-dependent memory and motor function in neuropilin 2–deficient mice. Transl Psychiatry. 2015;5(3):e521–e521. Available from: https://www.nature.com/articles/tp201517
24. Eisenberg C, Subramanian D, Afrasiabi M, Ziobro P, DeLucia J, Hirschberg PR, et al. Reduced hippocampal inhibition and enhanced autism-epilepsy comorbidity in mice lacking neuropilin 2. Transl Psychiatry. 2021;11(1):537.
25. Walz A, Rodriguez I, Mombaerts P. Aberrant Sensory Innervation of the Olfactory Bulb in Neuropilin-2 Mutant Mice. The Journal of Neuroscience. 2002;22(10):4025–35.

26. Afrasiabi M, Gupta A, Xu H, Swietek B, Santhakumar V. Differential Activity-Dependent Increase in Synaptic Inhibition and Parvalbumin Interneuron Recruitment in Dentate Granule Cells and Semilunar Granule Cells. The Journal of Neuroscience. 2022;42(6):1090–103.
27. Nóbrega-Pereira S, Kessaris N, Du T, Kimura S, Anderson SA, Marín O. Postmitotic Nkx2-1 Controls the Migration of Telencephalic Interneurons by Direct Repression of Guidance Receptors. Neuron. 2008;59(5):733–45.
28. Okuyama T, Kitamura T, Roy DS, Itohara S, Tonegawa S. Ventral CA1 neurons store social memory. Science (1979). 2016;353(6307):1536–41.
29. Tao K, Chung M, Watarai A, Huang Z, Wang MY, Okuyama T. Disrupted social memory ensembles in the ventral hippocampus underlie social amnesia in autism-associated Shank3 mutant mice. Mol Psychiatry. 2022;27(4):2095–105.
30. Pelkey KA, Chittajallu R, Craig MT, Tricoire L, Wester JC, McBain CJ. Hippocampal GABAergic Inhibitory Interneurons. Physiol Rev. 2017;97(4):1619–747.
31. Simon A, Oláh S, Molnár G, Szabadics J, Tamás G. Gap-Junctional Coupling between Neurogliaform Cells and Various Interneuron Types in the Neocortex. The Journal of Neuroscience. 2005;25(27):6278–85.
32. Oláh S, Komlósi G, Szabadics J, Varga C, Tóth E, Barzó P, et al. Output of neurogliaform cells to various neuron types in the human and rat cerebral cortex. Front Neural Circuits. 2007 [cited 2023 Dec 30];1:4.
33. Turrigiano GG, Nelson SB. Homeostatic plasticity in the developing nervous system. Vol. 5, Nature Reviews Neuroscience. European Association for Cardio-Thoracic Surgery; 2004. p. 97–107.
34. Marder E, Goaillard JM. Variability, compensation and homeostasis in neuron and network function. Nat Rev Neurosci. 2006;7(7):563–74.
35. Nelson SB, Valakh V. Review Excitatory/Inhibitory Balance and Circuit Homeostasis in Autism Spectrum Disorders. Neuron. 2015;87:684–98.
36. Booker SA, Vida I. Morphological diversity and connectivity of hippocampal interneurons. Cell Tissue Res. 2018;373(3):619–41.
37. Colmers WF, Bleakman D. Effects of neuropeptide Y on the electrical properties of neurons. Trends Neurosci. 1994;17(9):373–9.
38. Lunden JW, Durens M, Phillips AW, Nestor MW. Cortical interneuron function in autism spectrum condition. Pediatr Res. 2019;85(2):146–54.
39. Hitti FL, Siegelbaum SA. The hippocampal CA2 region is essential for social memory. Nature. 2014;508(7494):88–92.
40. Meira T, Leroy F, Buss EW, Oliva A, Park J, Siegelbaum SA. A hippocampal circuit linking dorsal CA2 to ventral CA1 critical for social memory dynamics. Nat Commun. 2018;9(1):4163.
41. Donegan ML, Stefanini F, Meira T, Gordon JA, Fusi S, Siegelbaum SA. Coding of social novelty in the hippocampal CA2 region and its disruption and rescue in a 22q11.2 microdeletion mouse model. Nat

Neurosci. 2020;23(11):1365–75.

42. Whitebirch AC, Santoro B, Barnett A, Lisgaras CP, Scharfman HE, Siegelbaum SA. Reduced Cholecystokinin-Expressing Interneuron Input Contributes to Disinhibition of the Hippocampal CA2 Region in a Mouse Model of Temporal Lobe Epilepsy. The Journal of Neuroscience. 2023;43(41):6930–49.
43. Aggleton JP, Nelson AJD. Distributed interactive brain circuits for object-in-place memory: A place for time? Brain Neurosci Adv. 2020;4:239821282093347.
44. Assous M, Martinez E, Eisenberg C, Shah F, Kosc A, Varghese K, et al. Neuropilin 2 Signaling Mediates Corticostriatal Transmission, Spine Maintenance, and Goal-Directed Learning in Mice. The Journal of Neuroscience. 2019 Nov 6 ;39(45):8845–59.
45. Bradfield LA, Leung BK, Boldt S, Liang S, Balleine BW. Goal-directed actions transiently depend on dorsal hippocampus. Nat Neurosci. 2020;23(10):1194–7.
46. Corbit LH, Balleine BW. The Role of the Hippocampus in Instrumental Conditioning. The Journal of Neuroscience. 2000;20(11):4233–9.
47. Kaminer J, Espinoza D, Bhimani S, Tepper JM, Koos T, Shiflett MW. Loss of striatal tyrosine-hydroxylase interneurons impairs instrumental goal-directed behavior. European Journal of Neuroscience. 2019;50(4):2653–62.
48. Holly EN, Davatolhagh MF, Choi K, Alabi OO, Vargas Cifuentes L, Fuccillo M V. Striatal Low-Threshold Spiking Interneurons Regulate Goal-Directed Learning. Neuron. 2019;103(1):92–101.e6.

Figures

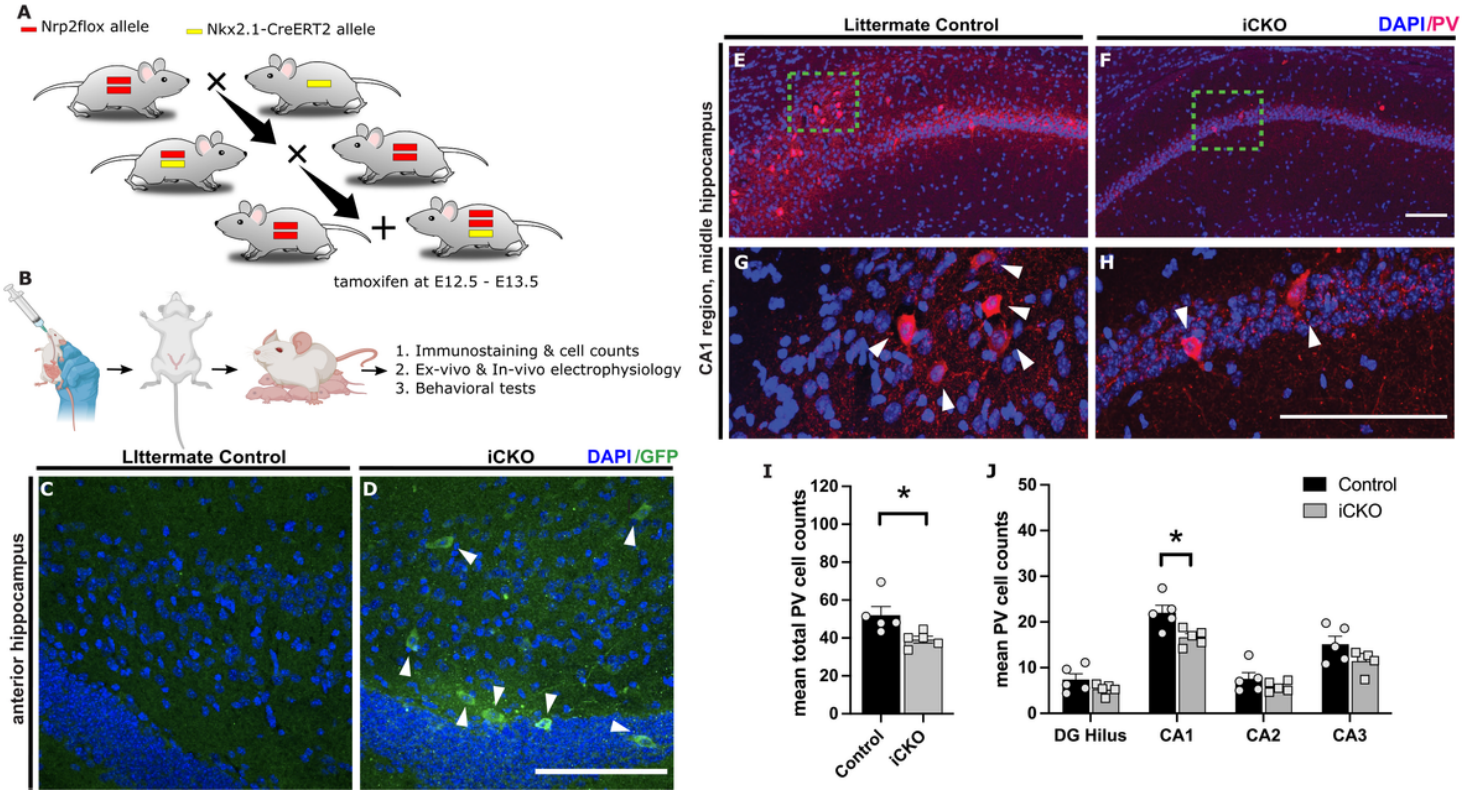

Figure 1

Developmental deletion of *Nrp2* leads to reduced numbers of parvalbumin (PV) expressing neurons in the hippocampus. A. Schematic illustrates the inducible conditional knockout strategy which allows *Nrp2* to be excised from neurons harboring transcription factor Nkx2.1 found in inhibitory neurons originating from the MGE in a spatiotemporal controlled manner. *Nrp2flox*mice were crossed with *Nkx2.1-CreERT2* mice to generate mice with and without *Nkx2.1-Cre* positive alleles. B) Timeline adopted for excising Nrp2 in Nkx2.1 expressing neurons at E12.5 and E13.5. Tamoxifen administered at E12.5 and E13.5 by oral gavage, pups were delivered by C-section then housed with a foster mom. C, D) Brain sections immuno-labeled with anti-GFP (green) in the anterior DG region demonstrate excision of Nrp2 (mutant cells). E-H) Immuno-labeled control (E,G) and iCKO (F,H) brain sections, respectively, with anti-PV (red) and DAPI (blue). G,H) High magnification images of green boxes in E and F, respectively. I) Quantification of total mean PV+ hippocampal cells. J) Quantification of the average number of PV+ cells by hippocampal region. n=5 animals/genotype. Error bars are ± SEM; two-way ANOVA, post-hoc Bonferroni for multiple comparisons: *p=0.0132 CA1 region, *p=0.0302 unpaired t-test overall hippocampus. Significantly fewer number of PV+ neurons found in hippocampus of iCKO compared to control mice. All scale bars: 100 µm.

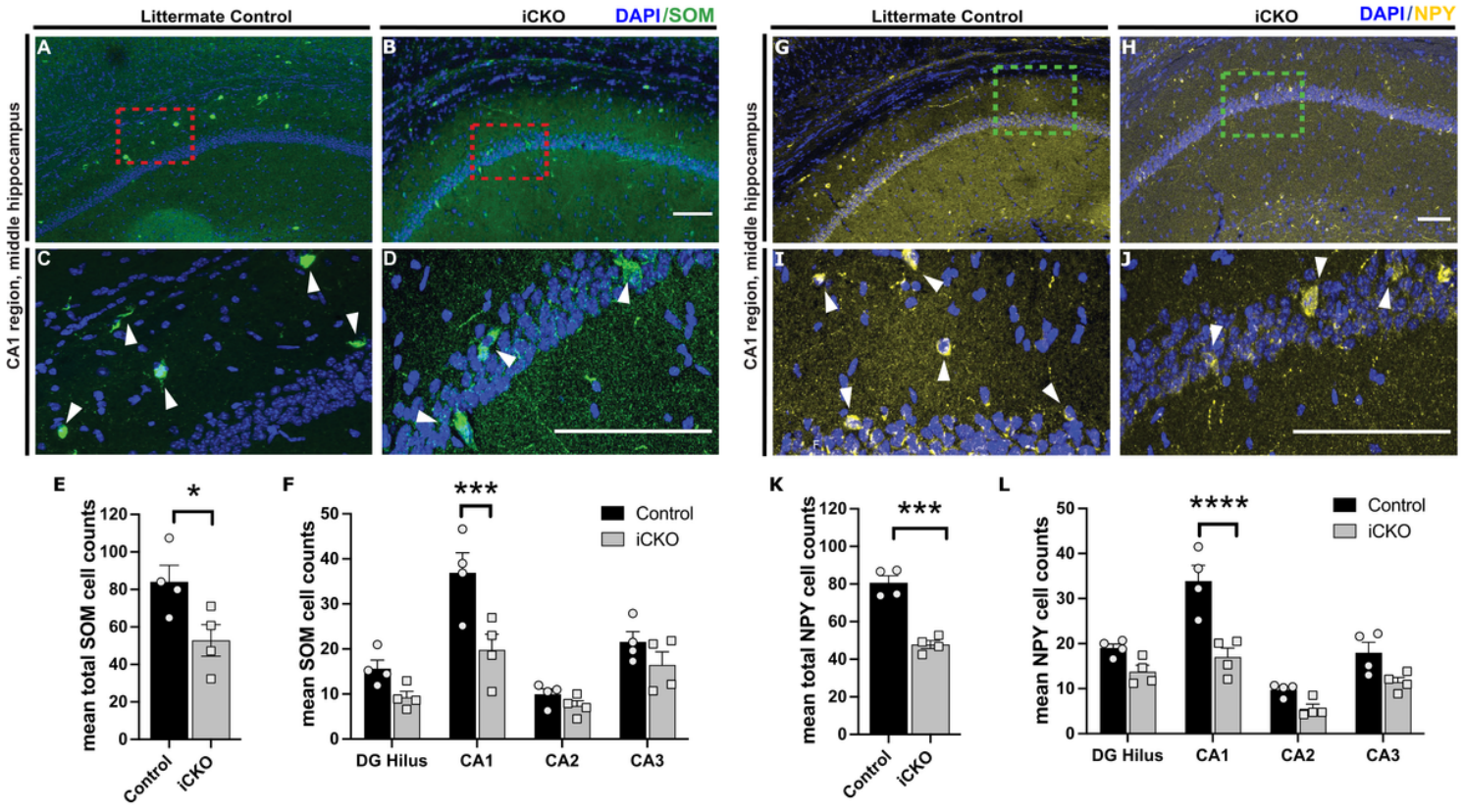

Figure 2

Deletion of *Nrp2* at an embryonic stage results in reduced numbers of somatostatin (SOM) and neuropeptide Y (NPY) expressing neurons in the CA1 region of the hippocampus. A-D) Immuno-labeled of littermate control (A,C,) and iCKO (B,D\) brain sections, respectively, with anti-SOM (green) and DAPI

(blue). (C,D) High magnification images of area in red boxes in A,B, respectively. Scale bars: 100 μm. E) Quantification of total mean SOM+ hippocampal cells. Error bars are ± SEM; unpaired *t*-test: *p=0.0426. Significantly fewer number of SOM+ neurons found in hippocampus of iCKO compared to control mice. F) Quantification of the average number of SOM+ cells by hippocampal region. Significantly lower SOM+ cell density found in CA1 region of iCKO mice compared to littermate controls; ***p=0.0004. n=4 animals/genotype. G-J) Immuno-labeled of littermate control (G,I) and iCKO (H,J) brain sections, respectively, with anti-NPY (yellow) and DAPI (blue). (I,J) High magnification images of area in green boxes in G,H, respectively. Scale bars: 100 μm. K) Quantification of total mean NPY+ hippocampal cells. Error bars are ± SEM; two-way ANOVA, post-hoc Bonferroni for multiple comparisons: ***p=0.0003. Significantly fewer number of NPY+ neurons found in hippocampus of iCKO compared to control mice. L) Quantification of the average number of NPY+ cells by hippocampal region. Significantly lower NPY+ cell density found in CA1 region of iCKO mice compared to littermate controls; ****p<0.0001. n=4 animals/genotype.

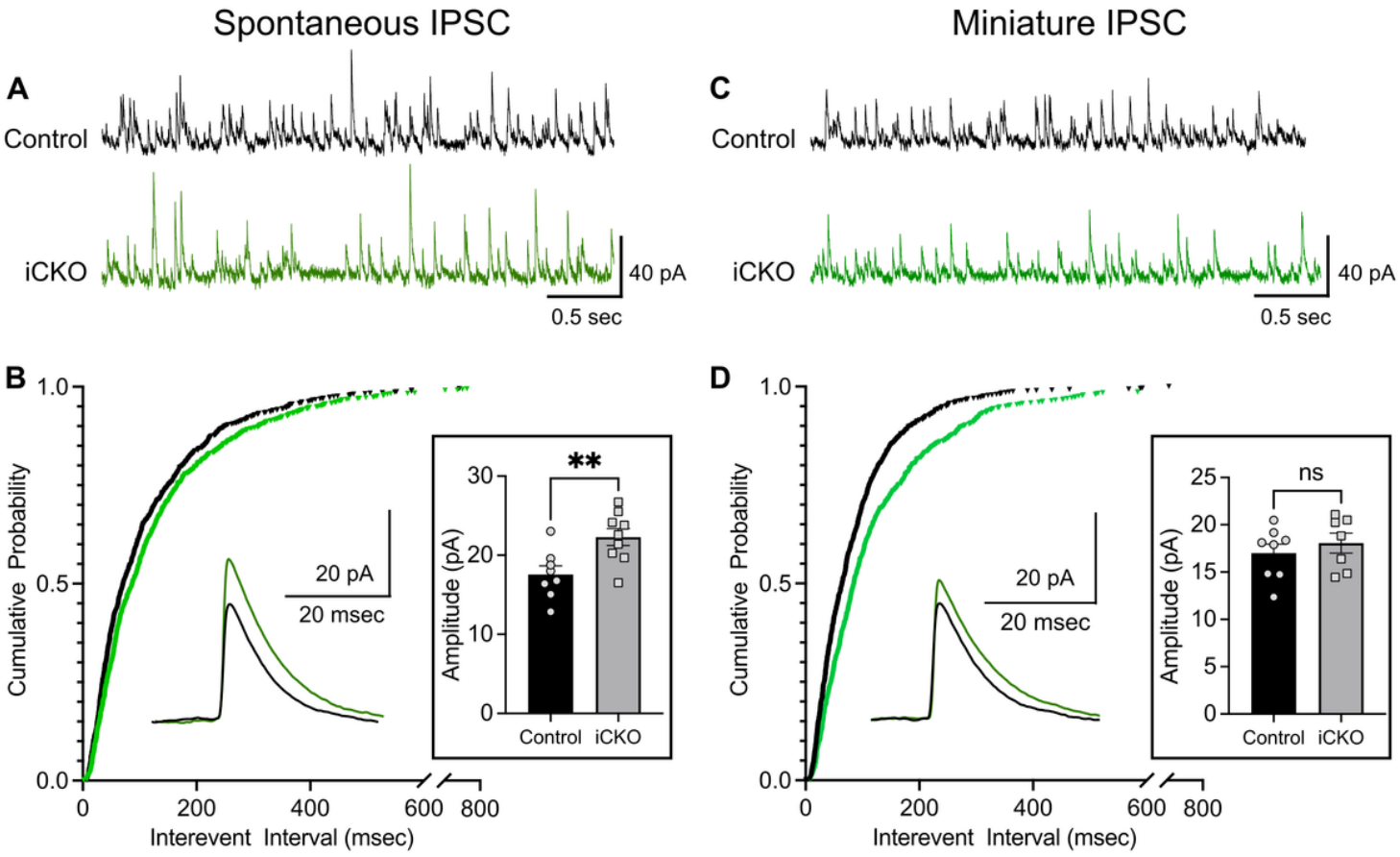

Figure 3

Reduced inhibitory synaptic inputs to CA1 PCs from iCKO mice

A) Representative spontaneous inhibitory postsynaptic current (sIPSC) recordings in control and iCKO mice. Note that events are less frequent in iCKO mice. B) Cumulative distribution of sIPSC interevent intervals show a right shift in iCKO mice suggesting a lower frequency of sIPSC compared to controls (n=

8-9 cells from 3 mice / group, p=0.0037, Kolmogorov-Smirnov test) . Insets: Representative average traces and summary data show the larger sIPSC amplitude in iCKO mice (p = 0.0071, unpaired t-test). C) Representative miniature inhibitory postsynaptic currents (mIPSC) in control and iCKO mice. D) Cumulative distribution of mIPSC interevent intervals show a right shift in iCKO mice indicating a lower frequency of mIPSC compared to controls (n= 7-8 cells from 3 mice/group, p<0.0001, Kolmogorov-Smirnov test) Insets: Representative average traces and summary data of mIPSC amplitudes in control and iCKO mice.

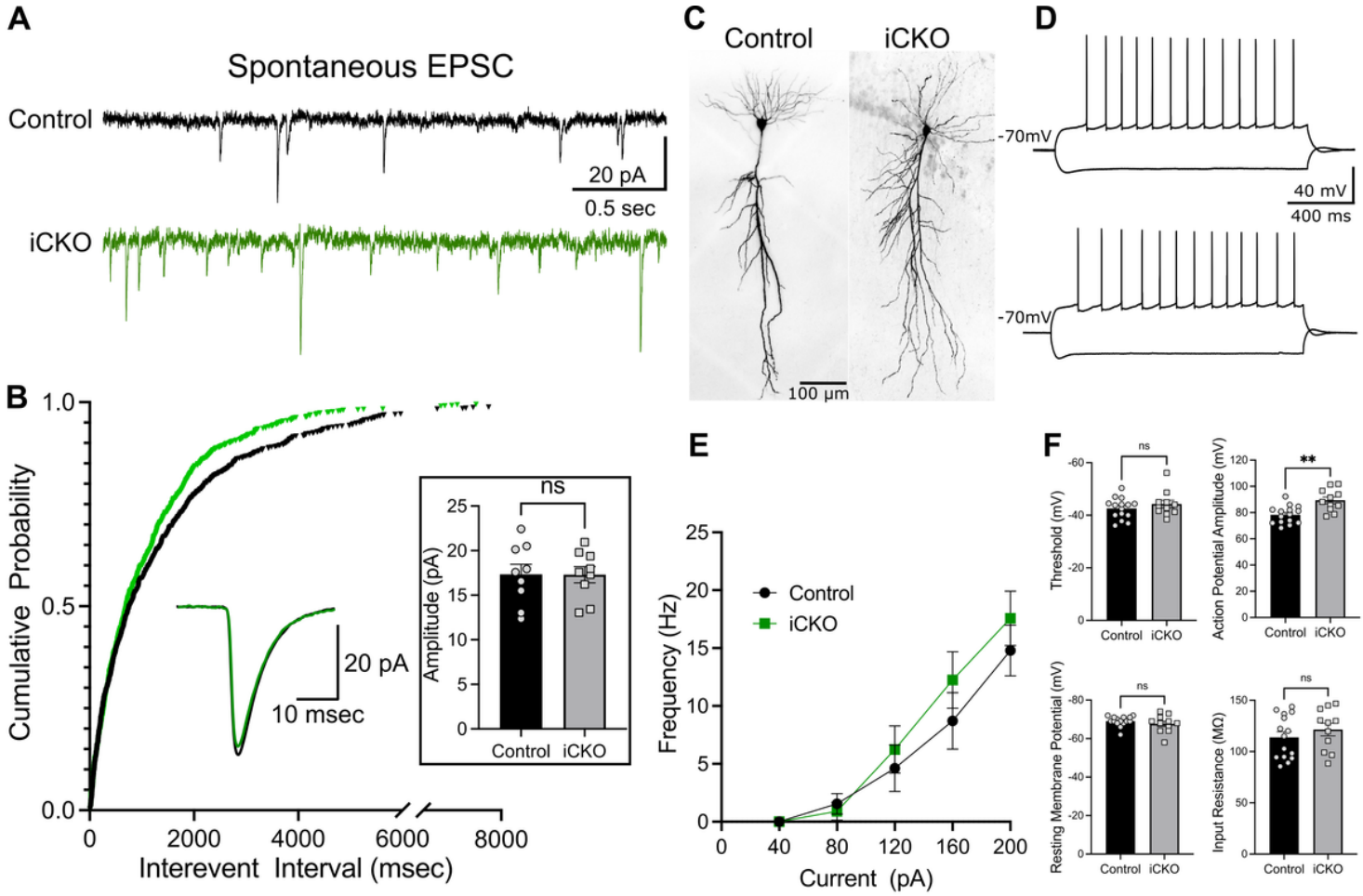

Figure 4

CA1 PCs from *iCKO* mice show changes in excitatory synaptic inputs but not in intrinsic active and passive properties.

A) Representative traces showing spontaneous excitatory postsynaptic currents (sEPSC) in control and iCKO mice. Note that events are more frequent in iCKO mice. B) Cumulative distribution of sEPSC interevent intervals show a left shift in iCKO mice suggesting a higher frequency of sEPSC compared to controls (n = 9 cells from 3 mice/group, p = 0.0243, Kolmogorov-Smirnov test). sIPSC amplitudes were not different between control and iCKO mice. C) Representative images of CA1 PCs filled during recordings. D) Membrane voltage response to hyperpolarizing (-200pA) and depolarizing (+200pA) step current injections from control (above) and iCKO mice (below). E) Summary plot of firing frequency in

CA1 PCs in response to increasing current injections. F) Histograms compare firing threshold, resting membrane potential, input resistance and action potential amplitude in CA1 PCs between control and iCKO mice.

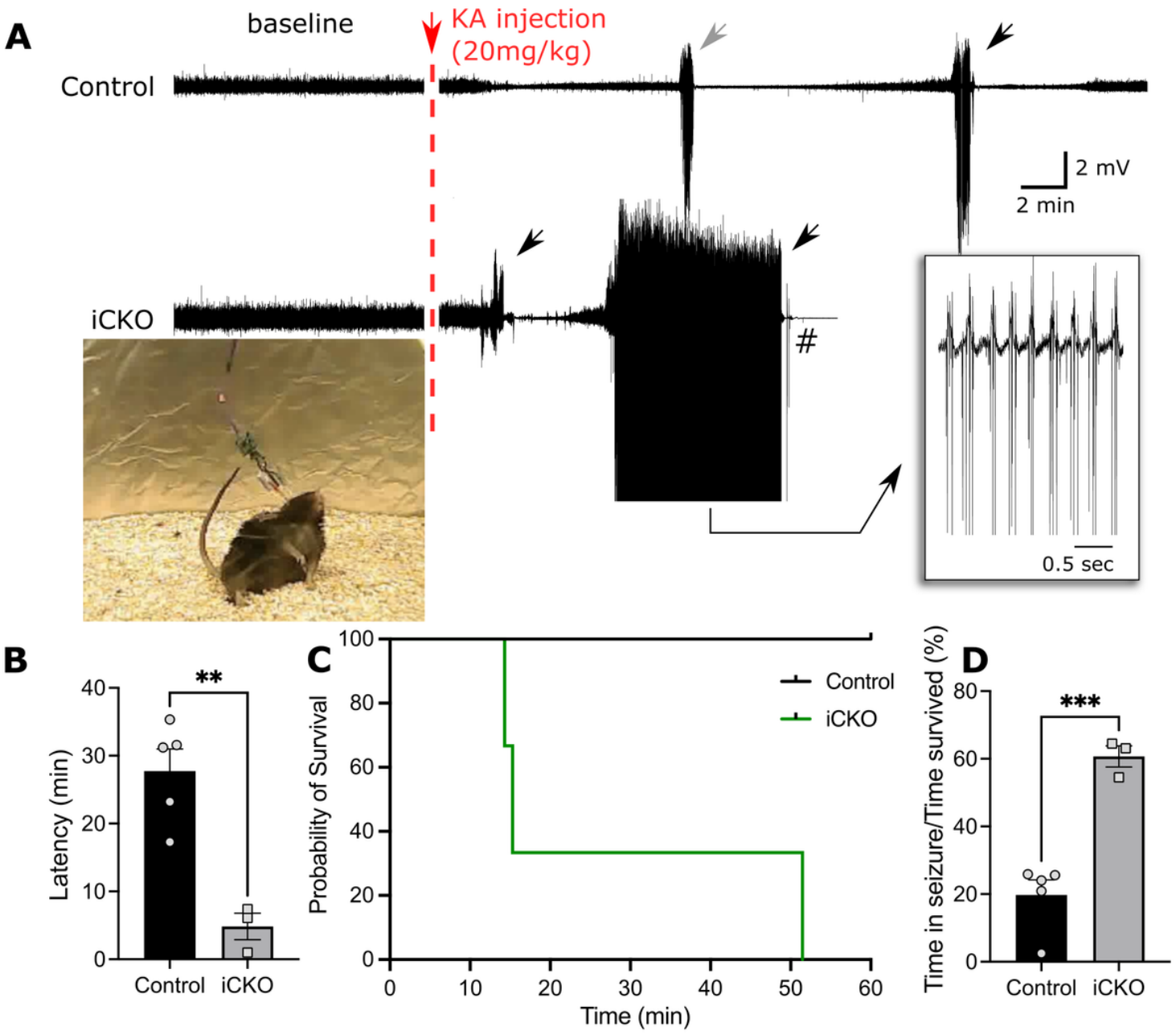

Figure 5

***Nrp2*$^{f/f}$*;Nkx2.1-CreERT2+* mice exhibit higher susceptibility to KA induced seizures.**

A) Example in EEG traces show the baseline activity and the development of seizures following KA induction (20mg/kg). Note that iCKO mice have a shorter latency to seizure onset and have longer lasting seizures. B) Quantification of latency to first convulsive seizures after KA induction shows that iCKO mice consistently had a short latency to convulsive seizures (n = 5 vs 3 mice, p = 0.0025, unpaired t-

test). C) Survival analysis showing iCKO mice succumbed more often to seizures whereas controls animals survived the first 60 minutes after induction (n = 5 vs 3 mice, p = 0.0042, Log-rank Mantel-cox test.). D) Ratio between total time spend in seizures to time survived after KA injection shows iCKO mice spent 60% of their time after KA induction in seizure compared to 19% in control mice.

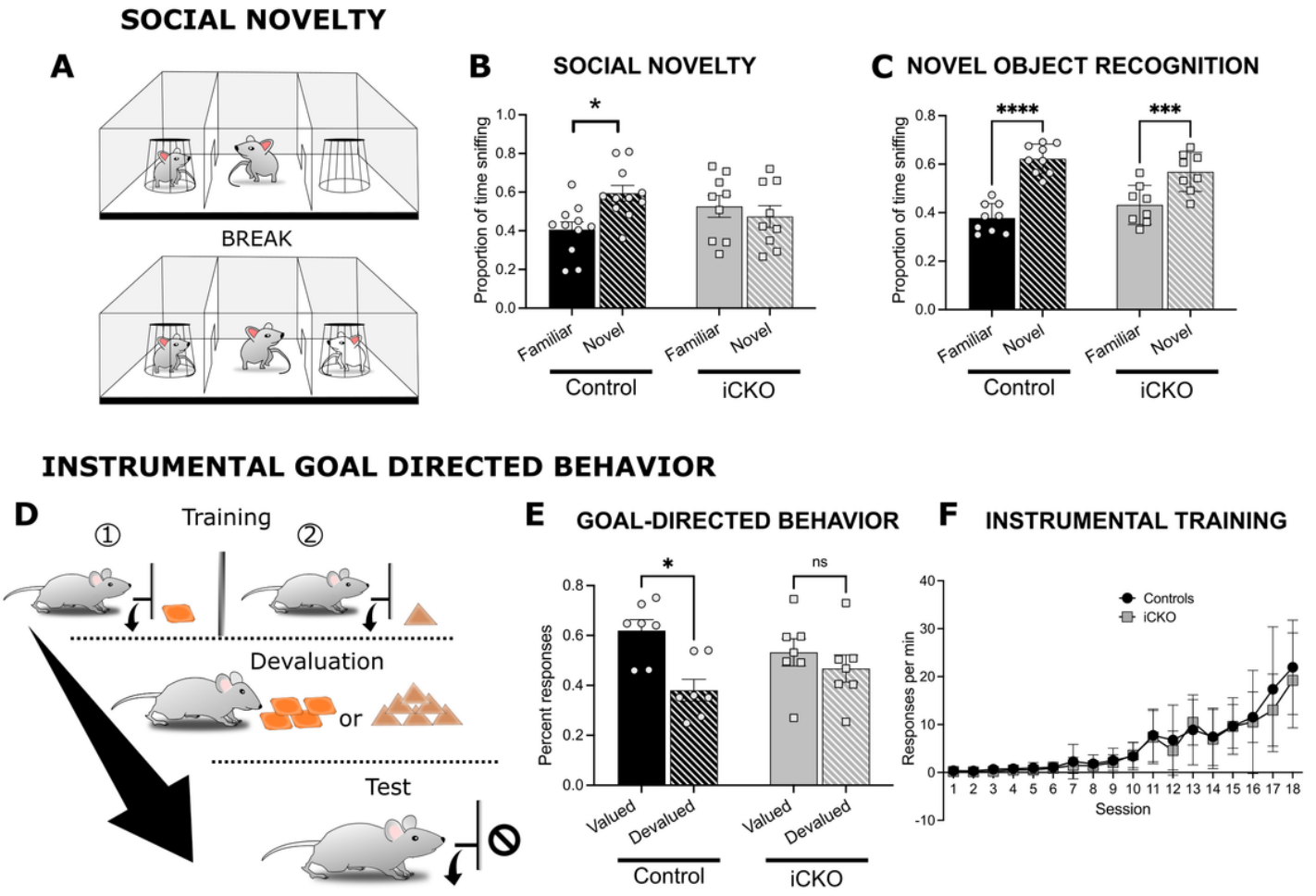

Figure 6

Social and goal directed behaviors are impaired in iCKO mice. A) Schematic of Social Novelty paradigm. B) Summary histogram compares time spent with novel compared to familiar mice in a social novelty test. Littermate controls spend significantly more time with a novel mouse compared to the lack of preference in iCKO mice (*p=0.011; n=11 controls, n=9 iCKO). C) Plot of time spent with a novel compared to the familiar object in a novel object task. Both littermate controls and iCKO mice spend more time exploring the novel object (**p=0.0011, ****p<0.0001; n=9 controls, n=8 iCKO mice. D) Schematic of operant chamber training and devaluation. E) Histogram of percent responses to the valued and devalued outcomes in iCKO mice and littermate controls during a goal-directed task. Control mice made significantly more actions associated with valued outcomes, whereas iCKO mice showed no difference in selecting actions associated with valued and devalued outcomes (**p<0.0001; n=7 controls, n=7 iCKO

mice. Error bars are ± SEM. F) Summary data of response rate during training on the lever press task shows no statistical differences between the groups.

Supplementary Files

This is a list of supplementary files associated with this preprint. Click to download.

- SubramanianEisenberg2024Supplementarymethods.docx
- SubramanianSupplementaryFiguresFinal.pdf